IJIE

INTERNATIONAL JOURNAL OF INTEGRATED ENGINEERING
ISSN: 2229-838X e-ISSN: 2600-7916

Vol. 18 No. 3 (2026) 366-388
https://publisher.uthm.edu.my/ojs/index.php/ijie

Diabetic Foot Ulcer Prediction Using Machine Learning Algorithms-Based on Multimodal Sensors Measurements

Sadik Kamel Gharghan[1,2]*, Ahmed Akeel Ali[1], Adnan Hussein Ali[3]

[1] *Middle Technical University, Electrical Engineering Technical College-Baghdad, IRAQ*
[2] *Middle Technical University, Technical Engineering College of Artificial Intelligence-Baghdad, IRAQ*
[3] *Middle Technical University, Institute of Technology-Baghdad, IRAQ*

*Corresponding Author: sadik.gharghan@mtu.edu.iq
DOI: https://doi.org/10.30880/ijie.2026.18.03.025

Article Info

Received: 11 October 2025
Accepted: 17 April 2026
Available online: 30 April 2026

Keywords

Decision tree, diabetic foot, biomedical sensors, machine learning, prediction, random forest, support vector machine

Abstract

Diabetic foot ulcers (DFUs) are a complication of diabetes that affects the feet. This occurs due to poor blood circulation and nerve damage from high blood sugar levels. DFUs are characterized by ulcers that heal slowly and increase the risk of infection. Delayed detection may lead to amputation. Therefore, early detection of DFU is critical. Most previous studies have relied on single-sensor data or small datasets, which limits their applicability. This study addresses this gap by integrating multimodal sensor data with ML algorithms for DFU prediction. In this paper, we propose a DFU prediction system that incorporates multiple sensors in a specific wireless sensor network (WSN). The sensors measure foot temperature, pressure, and humidity to assess diabetic foot health conditions. ESP32 microcontrollers instantly process sensor data for remote communication with smartphones. The measurements collected from physiological sensors were integrated with machine learning (ML) algorithms to predict DFU. Four ML algorithms were used: decision tree (DT), random forest (RF), k-nearest neighbors (KNN), and support vector machine (SVM). These algorithms classify and predict whether feet are healthy or unhealthy using multimodal sensor data. The data was divided into 80% training and 20% testing sets, and results were validated using 10-fold cross-validation. The accuracy, recall, specificity, AUC, F1 scores, and precision were evaluated for the implemented algorithms. The DT algorithm showed the highest accuracy, achieving 99.0% compared to other algorithms in this research and earlier studies. The integration of WSN and ML has proven valuable in classifying and forecasting DFU, confirming that the proposed method can enhance current diagnostic methods.

1. Introduction

The metabolic disease Diabetes Mellitus (DM) contains elevated blood glucose that develops from impaired insulin function or secretion, or both mechanisms, creating this disorder [1]. Diabetic foot ulcers (DFUs) stand among the most severe complications that arise from diabetes because they cause substantial disability to patients. Both peripheral vascular disease and trauma and neuropathy merge to form DFUs, which subsequently result in infections and hospital stays and potentially end with full or partial amputations [2]. The early recognition and control of diabetic foot complications risk factors remain essential to stop poor patient outcomes and improve health quality. Wearable equipment that measures physiological data and machine learning (ML) techniques has developed into strong monitoring tools for DFU conditions that enable rapid intervention approaches [3].

DFU is a severe complication of diabetes that affects the feet, harming nerves and blood vessels, resulting in loss of sensation, infections, and wound exposure; in advanced circumstances, the limb may require amputation [4]. Its major causes are elevated blood sugar for extended periods because of inadequate control of diseases [5]. Its symptoms include numbness, tingling, and burning in the feet, skin discoloration, swelling, cracks, blisters, sores, hair loss, bone and joint abnormalities, and loss of sensibility to pain, heat, or cold [6]. Traditional methods of diagnosis are to examine the feet frequently, notice shifts in the skin, nails, and toes, use systems to evaluate sensation and circulation, and inspect the wound samples [7]. X-rays, ultrasounds, and MRIs detect bone and vascular damage [8, 9].

The world currently has 642 million DM patients, which represents a projected increase to 800 million by 2045. DFUs represent a significant complication that develops in one-quarter of DM patients, leading to 40% to 70% of the cases where doctors must perform non-traumatic lower limb amputations throughout the world due to the occurrence of over a million such procedures yearly. Diabetes patients experience a yearly DFU development rate of roughly 2.5%, but among these patients, 14-24% require amputation procedures following diagnoses, and survival odds for diabetes patients with foot ulcers show a mortality range between 50% and 70% over five years. The recurring nature of DFUs affects 65% of affected patients during the 3-5 year period, resulting in sustained health-related challenges and financial expenses globally [10].

The progress made in DFU management has not eliminated the difficulties of predicting when DFUs appear. Present risk assessment of diabetic feet today depends primarily on physical evaluations and patient history recordings alongside evaluator subjectivity, which proves inconsistent outcomes [11]. The current predictive models face various limitations because they work with limited dataset quantities, insufficient feature identification, and restricted universal applicability. The research requires stronger data-guided approaches to use physiological sensor data in combination with advanced computational methods to improve the accuracy and reliability of DFU prediction systems [12]. Resolving these challenges is necessary to decrease the healthcare system's burden on DFU complications for patients and medical professionals.

WSN integration with AI significantly changes medical diagnostic and patient monitoring capabilities, alongside sports performance evaluation processes. WSNs in healthcare gather instantaneous physiological sensor data from sensors attached to the body or implanted inside bodies to monitor patients continuously and detect diseases early, as well as daily activities [13]. AI algorithms extract valuable patterns from collected medical data, which allows them to foresee potential health perils and aid in comprehensive disease diagnoses, including cardiovascular diseases, diabetes, and neurological disorders at high accuracy levels. Sports-based WSN wearables monitor athletes by tracking their biomechanics, movement patterns, physiological training, and competition responses [14]. AI analytics improved for athlete's permits performance development and injury prevention while creating personalized training programs from individual data points. The combination of WSN with AI technology brings automated choices, precise feedback, and real-time assistance, leading to improved patient care and performance enhancement for healthcare and sports sectors.

According to previous research, the prediction of DFU complications has been studied using different solutions that involve both ML approaches and sensor-based data. The researchers have applied support vector machines (SVM) [15, 16], random forests (RF) [17], k-nearest neighbors (KNN) [18], Naïve Bayes [19], and artificial neural networks (ANNs) [20, 21] as classification algorithms to evaluate skin temperature, plantar pressure, and blood flow physiological indicators. Some researchers have developed wearable technology [22, 23] to track DFU based on different sensors, such as pressure, temperature, and humidity. These investigation methods generate hopeful results yet encounter three main obstacles: working with restricted data, ignoring live predictions, and difficulties joining various sensor devices. Existing methodology restrictions emphasize developing new solutions beyond current operational limitations.

The scope of this study is to design and evaluate a complete system that integrates multimodal physiological sensors with ML algorithms through a wireless sensor network (WSN) for early DFU prediction. Unlike previous works, which often focus on one type of signal or limited datasets, our work emphasizes multimodal integration, real-time monitoring, and algorithmic comparison.

This research aims to predict and detect DFU in real time by merging the physiological sensor measurements with ML algorithms. Four well-known ML algorithms are applied, such as a DT rule-based model that splits data into branches for simple interpretation. RF is an ensemble method that combines multiple decision trees to improve stability and reduce overfitting. KNN is a distance-based classifier that predicts a class based on similarity to neighboring data points. SVM is a powerful classifier that finds the optimal hyperplane to separate classes in a high-dimensional space. Fig. 9 shows the ML algorithms flowchart implemented in Python used in this research. The algorithm operation consists of four phases: data preparation, running ML models, model evaluation, and the user interface.

The proposed design offers an integrated sensor system in a simple wireless sensor network (WSN) that monitors diabetic foot health through force, temperature, and humidity sensors while ESP32 microcontrollers process data. The physiological data collected from the foot is transmitted wirelessly in real-time via WiFi from the DFU monitoring unit to a smartphone, where it is subsequently processed and analyzed [24, 25]. In addition, a user interface such as the RemoteXY application enables users to monitor their foot health status and obtain early alerts. The system provides a complete, non-invasive foot health monitoring solution that is simple to use while having the potential to scale up benefits through enhanced predictive abilities. In addition, the integration of WSN with ML algorithms creates an efficient method to improve the diagnostic accuracy of the forecasting of DF. Wireless sensors collect physiological data from the patient's foot, then test and train ML algorithms. Four ML algorithms, DT, KNN, RF, and SVM, are applied to these sensor data to classify feet as healthy or unhealthy. The prediction algorithms are not only practical but can also be more reliable than traditional methods.

The contributions of this study can be summarized as follows:

1. Wireless sensor network-based physiological parameters were designed and implemented practically to collect physiological data from the foot, including temperature, skin moisture, and foot pressure.
2. Various ML algorithms, including KNN, SVM, RF, and DT, were trained and tested using physiological data to predict DFU accurately.
3. ML algorithms were evaluated based on several performance metrics to select the best algorithm that achieves higher prediction accuracy.
4. The adopted ML algorithms outperformed existing algorithms in previous articles, revealing the robustness of our models in the early diagnosis and forecasting of DF.

This paper has the following organizational structure: Section 2 presents an in-depth review of prior works that focus on diabetic foot prediction alongside their significant developments and encountered obstacles. The methodology consists of Section 3, which details information about data acquisition procedures before moving on to feature selection and ML model creation. Section 4 assesses the effectiveness of the methodology proposed throughout this work based on several performance metrics. The paper moves on to Section 5 to explore the study's results and the discussion. Section 6 compares the outcomes of this paper with related previous works in terms of several performance metrics. Section 7 includes conclusions that offer future research.

2. Literature Review

This section reviews prior studies on the topic and highlights recent contributions by researchers. It presents the limitations researchers faced and each study's advantages and disadvantages. Prediction of DFU using WSN involves relying on ML algorithms to develop predictive models to identify individuals at risk of developing complications of DF. These models aim to predict the probability of developing DFU by analyzing various medical data, allowing early intervention and prevention strategies. This helps healthcare actors make decisions to improve patient outcomes.

Wang et al. [26] introduced a system of shoes for tracking plantar pressure every day for diabetic patients, and the system can dynamically track plantar pressure and show variations in real-time on a mobile device. The main problems of current prototypes are poor long-term measurement stability, poorly developed system integration and packaging processes, and unreliable wired and wireless connections between sensors, batteries, and processing units. The study aims to create a convenient long-term monitoring system and a user interface for viewing and analyzing the distribution of plantar pressure of diabetic patients in real-time, allowing early prevention of foot ulcers and providing early warning to patients. A shoe system with an insole equipped with pressure sensors is used to monitor plantar pressure. Five classifiers were used to classify plantar pressure for three groups of patients: healthy individuals, diabetic patients without peripheral neuropathy, and diabetic patients with peripheral neuropathy. The forest Randomizer's accuracy was 94.7%, which indicates the system's usefulness for tracking diabetic patients' daily plantar pressure. The most important benefits of the device are low cost, and it displays changes in real-time on the mobile phone and transmits data wirelessly through Bluetooth, ensuring that they do not affect the user's gait. However, they are not appropriate for continuous observation in everyday life, which hinders a practical assessment of the risk of DFU.

Chauhan et al. [27] focused on using ML to diagnose the different stages of diabetes development in the lower extremities by analyzing the distribution of pressure collected using pressure-measuring insoles. The goal is to detect peripheral neuropathy early to predict the development of DFU. Plantar pressure measurements were recorded while participants walked, and the data were divided into three plantar regions. Furthermore, data were collected at the UNLV Diabetes and Endocrinology Clinic using supervised ML algorithms to predict diagnoses effectively. Participants were 110 from the prediabetes group, the group without peripheral neuropathy, and the group with neuropathy. The best-performing models, such as KNN and SVM, using different compression and non-compression features, achieved accuracies ranging from 94.0% to 100%, highlighting the effectiveness of the proposed ML approach. Early detection of diabetes complications such as peripheral neuropathy has been a primary focus, allowing timely treatment and prevention of further problems. Generalizability may be limited because the study used specific ML algorithms and features. Different algorithms or features may produce different results in other populations or settings. Haque et al. [28] discussed diabetic neuropathy (DN) and foot ulcers using EMG and GRF signals. The goal is to identify patients with DN and DFU, providing a potential solution to classify patients. In practice, the EMG and GRF signals were collected from DN, DFU, and control groups during walking, and feature extraction techniques were applied to extract relevant features from the signals. ML algorithms, such as KNN, SVM, etc., have been used to classify patients. The KNN algorithm showed high accuracy in identifying DN and DFU patients, as EMG analysis achieved 96.18% accuracy using specific features of muscles and 98.68% using ground reaction forces analysis. The application of ML has provided a potential solution for accurate patient identification using EMG and GRF parameters. Improved ML models can help diagnose and classify DN and DFU patients. However, the data consisted of three small groups, and therefore, further validation and testing on more extensive and diverse data sets are needed to ensure that the results can be generalized.

Ferreira et al. [29] focused on developing an AI-based system to detect people at risk of developing DFU. The system was used to avoid severe symptoms by intervening in real-time. The experiment was conducted on a group of 250 individuals with diabetes in a health institution in Minas Gerais, Brazil, focusing on neuropathy, deformities, and trauma to detect DFU. A Multi-Layer Perceptron Neural Network (MLPNN) was used. The system achieved good accuracy, with values ranging from 81.0% to 87.0%, indicating the effectiveness of the proposed system for detecting the disease. However, the generalizability of the results to a larger population was limited because the data were collected from a single health institution. Basiri et al. [30] discussed the challenges of DFU detection using deep learning (DL) to improve early detection and treatment. The study used a detailed protocol case report form (CRF) to collect patient data, developed in consultation with clinicians and researchers. The study generated a dataset of 269 patients with DFU and approximately 3700 RGB images and heat maps. The dataset and UNet architecture were demonstrated to be effective for DFU detection. Using EfficientNet as a feature extractor and UNet architecture achieved promising results of F1-Score 79% and MAP 86%, demonstrating the effectiveness of the dataset used in DFU analyses and DL. The paper found that more research is needed in the field of DL and thermal imaging to improve the performance of the proposed system to identify disease.

Cassidy et al. [31] proposed a system based on smartphones and artificial intelligence (AI) to achieve high-accuracy detection of diabetic ulcers. Diabetic ulcers and amputations pose a considerable health and economic burden, with high expenses for healthcare systems. The evaluation was performed on 81 diabetic patients. A total of 203-foot photographs were collected. Using a smartphone, they were analyzed using an AI system and compared to the judgment of clinical experts, with 162 images showing at least one ulcer and 41 showing no ulcer. The system showed an accuracy of 92.12%, a recall of 92.26%, and a specificity of 91.67%, indicating the possibility of automated detection and monitoring of DFU. Using a low-cost smartphone for automated ulcer detection indicates cost-effectiveness and accessibility for widespread implementation in healthcare settings. The study period was limited to September 2020 to January 2021, which may not capture long-term performance or changes in the AI system over long periods. Radunovic et al. [32] explored Moveo, a device that uses ML and sensors placed in the hand and foot to detect neuropathy. The goal is to identify neuropathy early. The device uses four sensors in addition to traditional electrical examinations (EDx), analyzes, and processes them via the cloud instantly, giving accurate results. The experiment had 23 participants. The device achieved an accuracy of 82.1%, with a recall of 78%, an F1 score of 82.88%, a precision of 88.46%, and a specificity of 87%, showing promise for home use. The device provides users with a quick diagnostic method, improving their experience of managing their health condition. It may depend on cloud computing technology and mobile applications, as any glitch in the system can affect the diagnosis. Sensors can be jammed or lost, leading to inaccurate readings.

Salih et al. [33] introduced a diabetes classification model that received an improvement through data preprocessing techniques using the PIMA Diabetes dataset. The methodology implements sequential operations beginning with outlier elimination and data filling in the first phase, then continues with normalization procedures in the second stage. Principal component analysis was employed to analyze features in their study. SVM, RF, Naïve Bayes, and DT were selected to classify the PIMA dataset. Tests showed that an accuracy of 89.86% was achieved during training with 80% of the available data. The feature selection approach was used to merge with the classification system to achieve these results. The research by Fadhel et al. [34] focused on hardware accelerator-based automatic classification between normal and abnormal DFU. The authors present the DFU_FNet Convolutional Neural Network (CNN) as a lightweight feature extraction model for SVM and KNN classification while introducing the DFU_TFNet CNN for deep network analysis of hardware effectiveness. DFU_TFNet surpassed all other networks, including AlexNet, VGG16, and GoogleNet, evaluating 99.81% accuracy and 99.38% precision alongside 99.25% F1-score and 99.76% recall performance. Throughout the study, the researchers evaluate which devices, between GPUs and FPGAs, work best for real-time processing, although GPUs complete computations more rapidly, FPGAs minimize power consumption.

Rathore et al. [35] enhanced DL model interpretations for DFU labeling and localization work that maintains clinical validity. The adopted method in this work integrates explainable AI approaches in healthcare AI systems to establish clinical trust while making systems more easily usable for medical staff. Six advanced models, including Xception and DenseNet121 alongside ResNet50, InceptionV3, and MobileNetV2, as well as Siamese Neural Network (SNN), undergo assessment through interpretability techniques SHAP and LIME, and Grad-CAM. The SNN stood out among the models by reaching 98.76% accuracy alongside 99.3% precision, 97.7% recall, 98.5% F1-score, 99.2% specificity, and 98.6% area under the curve (AUC) in performance results. Gudivaka et al. [36] presented a state-of-the-art ML protocol for DFU classification. Reinforcement learning is an effective cost-saving strategy that improves DFU image analysis and classification to support healthcare decisions and risk evaluations. The model successfully classified data with an accuracy reaching 93.75%, a specificity of 81.03%, an F1 score of 84.09%, a recall of 86.93%, and a precision of 81.43%. The cluster-based analysis achieved classification efficiencies between 71% and 98.2%. The developed diagnostic system provides better DFU identification capabilities and represents a cost-effective alternative to conventional diagnostic approaches.

Wearable physiological sensors and ML techniques have emerged as powerful tools for early DFU monitoring. Previous studies explored individual parameters such as pressure, temperature, or blood flow using ML algorithms. However, these approaches often relied on limited datasets or single-sensor modalities, which restricted their applicability. Unlike previous research, our study introduces a novel contribution by merging multiple parameters (temperature, pressure, and humidity) with modern ML algorithms to achieve real-time and reliable DFU prediction.

The novelty of this work is that we combine a WSN with the latest ML algorithms to assess multimodal DFU, allowing us to detect it earlier and evaluate it in a more detailed manner than traditional or single-sensor approaches do. In contrast to the earlier research that usually involves the one-parameter analysis, our method integrates various sensor data with ML algorithms to forecast the complications of DFU, which can provide a more global picture of patient health conditions.

3. Materials and Methods

This section includes the system architecture, hardware components, power management, Remote XY application, software architecture, gathering of multimodal sensor data, machine learning algorithms, and system evaluation, as follows:

3.1 System Architecture

The method proposed in this research measures physiological data from the foot. An array of sensors is used to measure skin temperature, humidity, and plantar pressure in different areas of the foot. These include two DHT22 temperature and humidity sensors and eight pressure sensors (FSR). The measured data is then collected and processed using the ESP32 microcontroller, which sends the data via WiFi. The data will be received by a smartphone containing an application through which sensor readings are displayed. In addition, data is collected for healthy and unhealthy people to train various ML algorithms to predict the possibility of developing DFU in a patient. Therefore, the proposed method combines sensors, electronics, smartphone applications, and ML algorithms to monitor conditions. Foot and early prediction of DFU to help treat it and prevent its complications, as shown in Fig. 1.

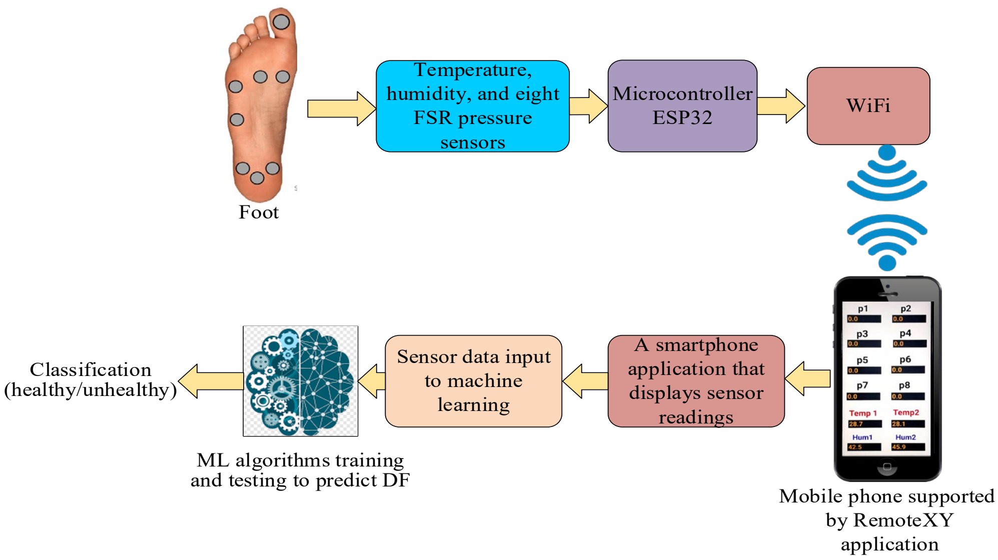

Fig. 1 *The architecture of the DF-based ML algorithms using WSN*

3.2 System Hardware

The electronic diagram shows the proposed system as in Fig. 2, where the proposed solution includes WSN. These sensors are strategically placed to collect relevant data from the patient's foot, consisting of 8 force sensors (Fig. 2, Part A) in slippers and two temperature and humidity sensors (Fig. 2, Part B). In addition to using an ESP32 microcontroller (Fig. 2, part C), it processes the data obtained from the WSN. The microcontroller contains WiFi with a frequency range of 2412-2484 MHz. After processing the data and calculating the pressure, temperature, and humidity values, the data is sent to the Android phone via a smartphone application designed by the RemoteXY website. Six high-resolution 12-bit analog input ports, from pin 3 to 8, were used to input the power sensors. In addition, temperature and humidity sensors can be connected using digital inputs 31 and 30. In addition to the I2C SCL and I2C SDA pins, these pins were used to connect the other two power banks by converting an analog-to-digital converter (ADC) using the ADS1115 module (Fig. 2, part D), also 12 bits, via programming. Fig. 3 shows the final circuit design model. The electronic components of the system are explained in the following subsections.

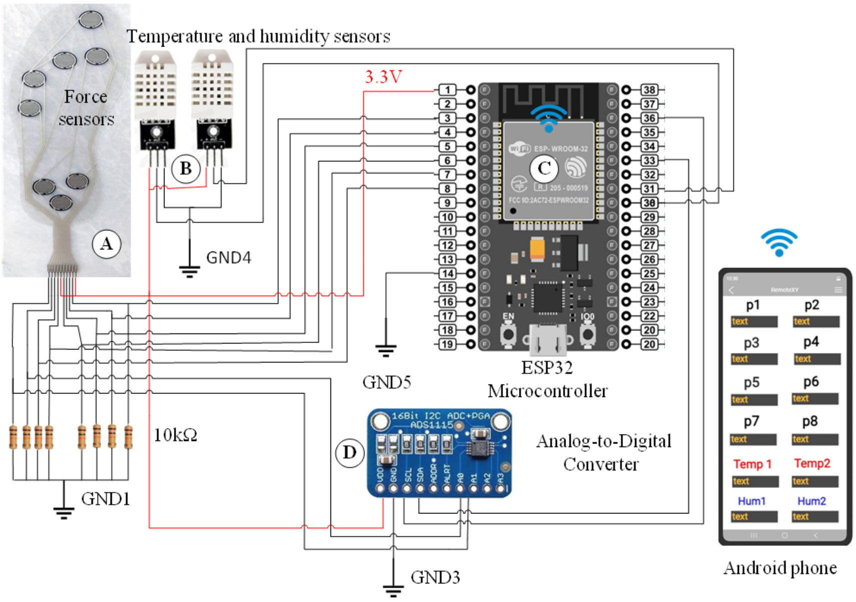

Fig. 2 *Schematic diagram of DFU based on WSN*

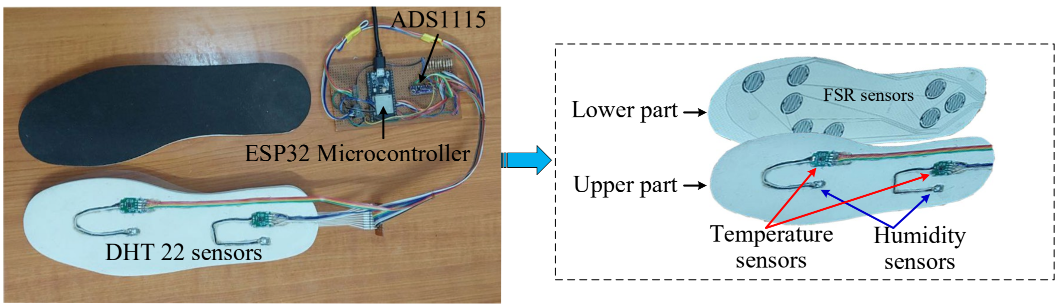

Fig. 3 *Snapshot of the hardware of the DFU based on WSN*

3.2.1 FSR Sensor

The force sensor shown in Fig. 2 (part A) is a variable resistance. The value of this resistance changes depending on the degree of pressure on it. One of the ANALOGE sensors lets us know the amount of pressure generated per unit area. For us to be able to read the values of this change through the analog ports, the change entering the analog ports must be a variable voltage and not resistance. Voltage divider technology is used to read this type of sensor. Assuming a VCC voltage source and two resistors, R and FSR, the two resistors were connected in series, as in Fig. 4.

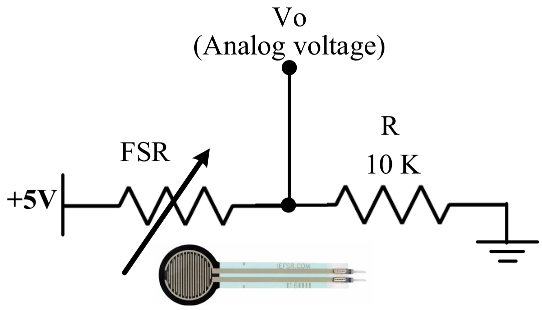

Fig. 4 *Electronic circuit voltage dividers*

This law is one of the essential laws in electrical circuits, as it can produce a lower voltage than the voltage source by changing the value of the resistors. However, used to read the amount of voltage on the force sensor, as in Equation (1). In this case, FSR will be the force sensor, and R will be a fixed resistance. When pressing the force sensor, its resistance will change, and the voltage value will change equally to change the resistance. In this way, current from the sensors can be obtained, which depends on the change in the resistor.

$$VO = VCC\frac{R}{R + FSR} \tag{1}$$

where VO represents the voltage output. VCC represents the Voltage Common Collector. R represents fixed resistance. FSR represents Force Sensor Resistance.

Eight FSR sensors were selected to capture pressure distribution across the plantar regions, while two DHT22 sensors were placed on the toe and heel areas to measure localized skin temperature and humidity. This arrangement allows multimodal physiological monitoring. Sensors were calibrated using known weights, as shown in Fig. (5).

Fig. 5(a) shows the calibration process of the FSR force sensors. While, Fig. 5(b) illustrates the calibration curve for the FSR force sensors used in WSN, which is the relationship between the weight in kilograms and the voltage in volts. The graph includes data points represented by black dots that were calculated using different weights and readings recorded in volts, ranging from 0.5 to 2.8 volts, and a blue line based on the data points. It ranges from 0 to 12 kilograms. The curve starts in the lower left corner of the graph and rises sharply as it progresses to the right, indicating an exponential-like increase in weight with effort. The curve calibration equation was calculated as shown in Equations (2), (3), and (4). In addition, the parameter values of Equation (3) are illustrated in Table 1, yielding Equation (4). Equation (4) was used in the proposed method's measurement algorithm.

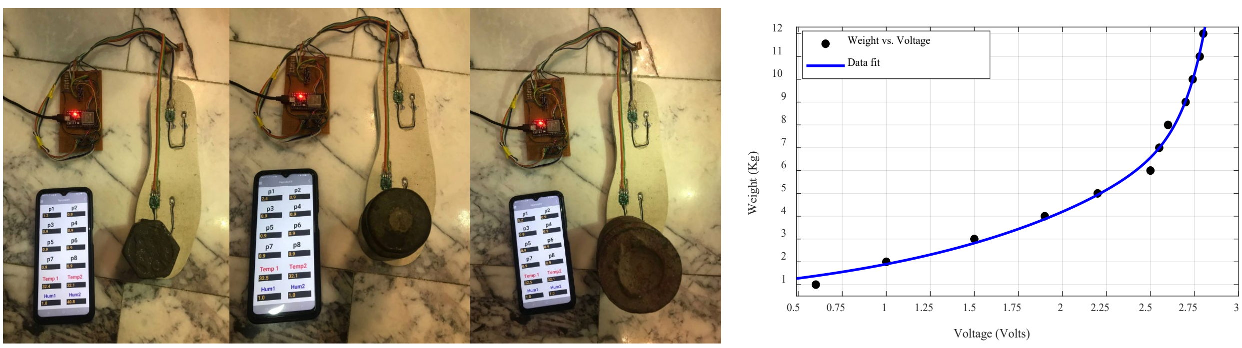

(a) **(b)**

Fig. 5 *Calibration of the FSR sensor (a) Process with different weights; and (b) Exponential curve fitting showing load–output relation for accurate pressure measurement*

Table 1 *Exponential equation parameters concerning their values*

Parameters of Exponential Equation	Exponential coefficient value
a	0.8606
b	0.7913
c	4.804×10-10
d	8.158
Correlation coefficient (R^2)	0.99434
Root Mean Square Error (RMSE)	0.318
Sum of squared error (SSE)	0.8088

$$f(x) = ae^{bx} + ce^{dx} \tag{2}$$

where *f(x)* is the weight measured in kilogram and *x* is the voltage measured in Volts.

$$W = ae^{bV} + ce^{dV} \tag{3}$$

$$W = 0.8606\, e^{\,0.7913\times V} + 4.804 \times 10^{-10} e^{8.158\times V} \tag{4}$$

3.2.2 DHT 22 Sensor

A sensor is used to measure temperature and humidity. The output of a calibrated digital DHT22 signal. It uses exclusive digital signal collection and humidity sensing technology, ensuring reliability and stability. Its sensing elements are connected to an 8-bit computer chip. Each sensor in this model is temperature-compensated and calibrated in a precision calibration chamber, and the calibration coefficient is saved in the program type in OTP memory [37]. Upon detection, the sensor cites the parameter from memory. The small size and low consumption enable the DHT22 to be suitable for all applications. A single row packed with four pins makes the connection very convenient, as presented in Fig. 2 (part B).

3.2.3 ESP32 Microcontroller

ESP32-WROOM-32 is a CPU. It has powerful, universal WiFi and Bluetooth, targeting various applications, from low-power sensor networks to the most demanding tasks. The embedded chip is designed to be scalable and adaptable. There are two individually controllable CPU cores, and the CPU clock frequency is user-adjustable from 80MHz to 240MHz. The chip also has a low-power coprocessor that can be used in place of the CPU. Save power while performing tasks that do not require a lot of computing power, such as monitoring devices [38].

The ESP32 integrates a rich set of hardware, such as capacitive touch sensors, SD card interface, Ethernet, high-speed SPI, UART, I2S, and I2C. WiFi allows for an extensive physical range and a direct Internet connection through a WiFi router. In contrast, Bluetooth lets users connect easily to the phone or stream from its low-power features [39]. The deep-sleep current of the ESP32 chip is less than 10 µA, making it suitable for electronic applications. Battery-operated and wearable [40]. The unit supports a data rate of up to 150 Mbps and 20 dBm of power at the antenna to ensure the most comprehensive physical range, as presented in Fig. 2 (part C).

3.2.4 ADS1115 Module

The ADS1115 Module can connect an external analog-to-digital converter (ADC) to a processor, such as ESP32 to measure analog signals. The ESP32 contains internal ADCs that can be used as analog inputs, 15 in number. However, not all can be used when using the built-in WiFi with the chip. Only six inputs are available, so this module allowed us to add four analog inputs [41].

The ADS1115 provides four 16-bit ADCs, 15 bits for measurement, and one for marking. The ADS1115 is communicated via I2C, so it is easy to read. It has four addresses, which are selected by connecting the ADDRESS pin. The benefit of using an ADC such as the ADS1115 is that it obtains greater accuracy and reduces the burden on the processor. In addition, in some configurations, it is possible to measure negative voltages. The ADS1115 has two measurement modes: single-ended and differential. In single-ended mode, it contains four 15-bit channels. In differential mode, use two ADCs for each measurement, reducing the number of channels to 2. However, they have the advantage of measuring negative voltages and better noise immunity, as presented in Fig. 2 (part D).

3.3 Power Management

Since the proposed system includes several sensors, we have carefully considered the power consumption of each of them, as it is illustrated in Table 2. The ESP32 microcontroller (120 mA) consumes the largest portion of all current draw, the two DHT22 humidity/temperature sensors (3 mA total), eight FSR sensors (1.76 mA in total), and the ADS1115 ADC consume the smallest portion of all current draw (0.15 mA). This would give a total active current consumption of about 124.91 mA at 3.3 V of supply voltage, which is a rechargeable lithium-ion battery of 4,800 mAh capacity (3.7 V) would give a theoretical continuous operating battery life time of:

$$Battery\ life = \frac{4{,}700\ mAh}{124.91\ mA} \approx 38\ hours$$

This amounts to approximately 1.5 days of continuous monitoring, which is adequate in short-term diagnostic sessions or daily use. Practically, the working battery life will likely be higher since the ESP32 supports deep sleep and duty cycling, at which point the system will only be awake at specific intervals to gather and send data instead of operating at maximum power. With this approach to power management, it was possible to extend the battery life to a few days, and this would depend on the frequency of the sampling and the intervals between the wireless transmissions.

Moreover, the system will have a rechargeable battery that can be easily recharged using either USB or wireless charging units, which will make the system sustainable and minimize maintenance processes. Even more energy-efficient features, e.g. adaptive sampling (recording only when abnormal patterns are detected) and low-power communication protocols (e.g., Bluetooth or LoRa, rather than constant Wi-Fi) may be further improved the operating time.

Table 2 *Power consumptions of the components of the DFU system at 3.3 V of supply voltage, with a 4,800 mAh/3.7 V rechargeable lithium-ion battery*

Component/parameter	Active current consumption (mA)
ESP32	120
DHT22	1.5x2 sensors=3
FSR	0.22x8 sensors=1.76
ADS1115	0.15
Total current	124.91 mA
Battery life	=Battery capacity/Active current consumption
	=4,700 mAh/124.91 mA= 38 hours

3.4 Remote XY Application

RemoteXY is an easy-to-create and use GUI on remote devices for control via smartphone or tablet. This system includes a remote GUI editor, available at remotexy.com, and the RemoteXY mobile app that allows one to connect to and control the remote devices using a graphical interface. A distinctive feature of the RemoteXY system is that the interface structure is stored in the controlling device, so there is no need to interact with servers to download the interface. Instead, the architecture is transferred to the mobile application directly from the controlling device [42]. With one mobile application, one can manage all devices, as there is no limit to the number of devices that can be controlled.

RemoteXY supports various connection methods, including Internet connection via a cloud server, WiFi connection as a client or access point, Bluetooth connection, Ethernet connection via IP or URL, and USB OTG connection (only available for Android devices) [43]. In addition, it supports ESP boards (ESP8266 and ESP32), STM32F1 boards, and ChipKIT boards (UNO32, uC32, and Max32). RemoteXY is available on various mobile operating systems, including Android and iOS. RemoteXY supports integrated development environments (IDEs) and related Arduino boards, including UNO, MEGA, Leonardo, Pro Mini, Nano, MICRO, and compatible AVR boards. In this paper, RemoteXY was used to support the ESP32 microcontroller. Fig. 6 shows the website from which the application was designed.

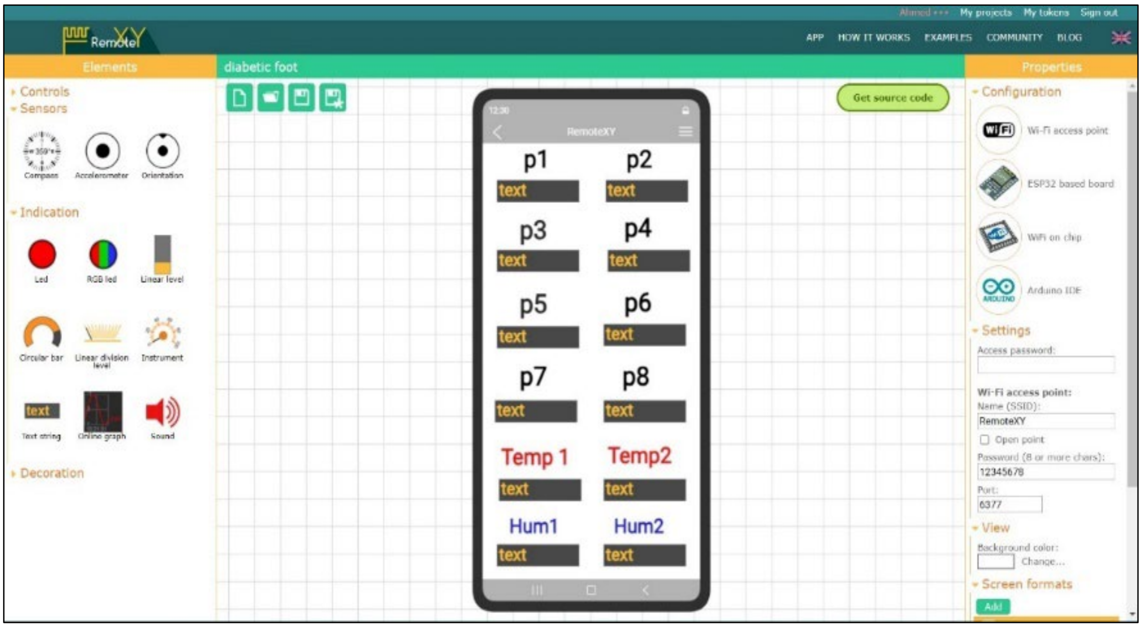

Fig. 6 *Website for RemoteXY*

3.5 Software Architecture

DFU detection using electronic circuits relies on a set of electronic components and software to analyze sensor data. Fig. 7 shows the flowchart of the proposed algorithm, using C++ to detect DFU. The following steps explain how the circuit detects DFU from the initial setup to display the processed data via the RemoteXY interface.

1. The sketch starts the code first, and the necessary libraries, such as RemoteXY, WiFi, DHT, and Adafruit_ADS1X15, are loaded [44]. These libraries provide the application's basic functionality.
2. The WiFi network is configured. The WiFi connection has been configured using the service set identifier and access point password to connect with RemoteXY. This connection allows the user to control and exchange data remotely.
3. RemoteXY has also been configured. RemoteXY server port and other connection settings are configured to enable remote control of the application.
4. Then, both sensors and serial communication are initialized. The input pins are assigned to the force sensors, and the DHT22 temperature and humidity sensors are configured. The serial communication is set at a baud rate 9600 to facilitate debugging and recording data.
5. After the preparation phase is completed, the main loop initiates.
6. The application's main loop is the running task, which handles RemoteXY events.
7. Read sensor data from various sensors (i.e., force, temperature, and humidity). In this step, the force applied by the foot on the shoe is measured at eight points, with six inputs connected directly to the ESP32 microcontroller and the other two through the Adafruit ADS1115 ADC before reaching the ESP32 microcontroller. The temperature and humidity data are measured directly from two DHT22 sensors.
8. Then, sensor data are processed and converted into appropriate formats to be stored in the RemoteXY variables.
9. The RemoteXY interface is then updated to display the sensed and processed new data. The program returns to step 6 to repeat the RemoteXY operation sequence.

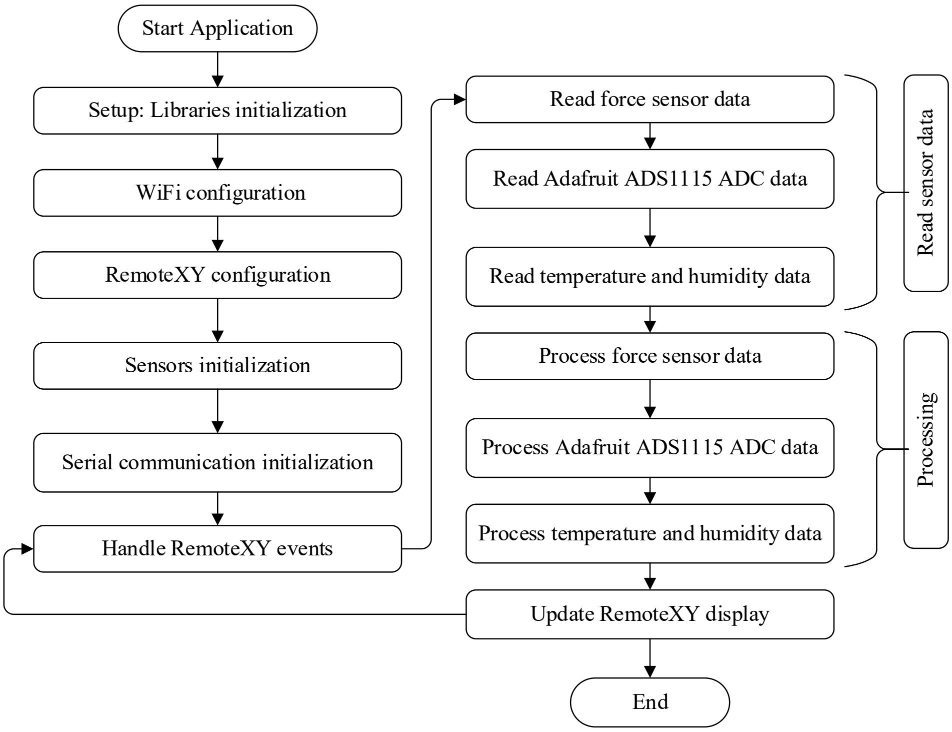

Fig. 7 *Flowchart of the program used in WSN*

3.6 Collection of Sensor Data

Data is collected through the WSN. This includes plantar pressure in eight areas of the foot to measure the distribution of pressure, temperature, and humidity of the skin in the toe and heel areas. Data was collected from 300 people with type 1 and type 2 diabetes. Healthy and unhealthy feet were defined by clinicians based on standard diagnostic criteria, including circulation tests, neuropathy assessment, and clinical examination. Inclusion criteria were confirmed diabetes diagnosis and ability to walk unaided. Exclusion criteria included severe deformities or other foot diseases. Ethical approval was obtained from the institutional ethics committee, and informed consent was obtained from all participants. 150 samples had healthy feet, and 150 samples had unhealthy feet. In addition, those aged from 30 to 70 years were taken from males and females. 80% of the data (240 samples) was used for training, and 20% (60 samples) was used to evaluate the system's performance using various performance measures. These percentages were chosen under the study [45]. This percentage was used to create a balance in the data, and most research relies on this percentage to achieve the best performance. During data collection, patients wore slippers with embedded sensors. Sweat, movement, and shoe interference were noted as potential influencing factors. The ESP32 microcontroller with WiFi provided portability. Patients reported the system as lightweight and comfortable. As an example, the data of the sensor measurements was taken from six volunteers, of whom three were unhealthy and the other three were healthy, as demonstrated in Table 3. Fig. 8 illustrates the collected foot pressure, temperature, and humidity data.

Table 3 *A database is used to train and test the system*

P_No	p1 (kPa)	p2 (kPa)	p3 (kPa)	p4 (kPa)	p5 (kPa)	p6 (kPa)	p7 (kPa)	p8 (kPa)	Temp1 (°C)	Temp2 (°C)	Hum1 (%)	Hum2 (%)	Cls
#1	2.5	4.8	5.1	5.5	4.5	12	10.7	21.9	30.8	31.7	48	49	0
#2	5.8	10.7	10.4	10.5	8.4	15.8	15.5	22.4	30.9	30	63.1	65.3	0
#3	2.7	4.8	4.9	5	5.1	10.7	11.7	23.7	34.1	35.1	58.3	58.3	0
#4	7.7	15.6	6.1	9.5	13	13.5	9.9	22	32	34	94.5	91.5	1
#5	4.8	5.4	12.6	10.4	14.5	11.2	6.1	22.2	35.3	36.3	55.1	50.1	1
#6	6.5	8.9	10.3	13	9.7	14.3	13	25.4	31.2	33.2	63.7	69.7	1

P_No: patient number; p1, p2, p3, p4, p5, p6, p7, p8: Plantar pressure; Temp1, Temp2: Skin temperature; Hum1, Hum2: Skin humidity; 0: Healthy foot; 1: Unhealthy foot; Cls: Classification

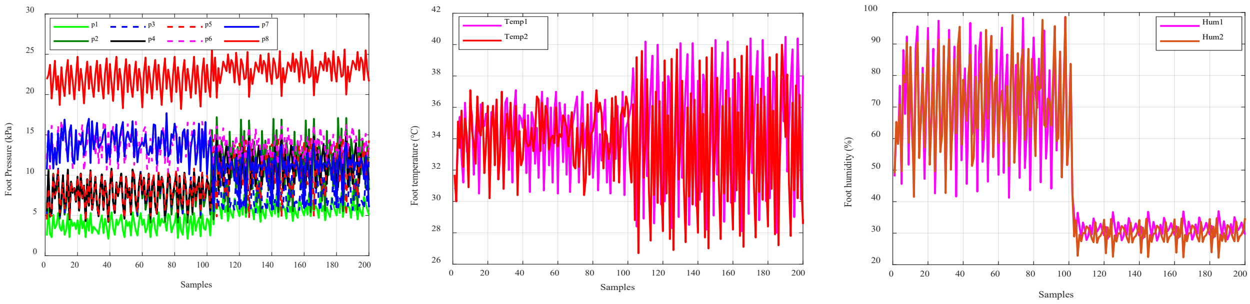

(a) **(b)** **(c)**

Fig. 8 *Foot collected data (a) Pressure; (b) Temperature; (c) Humidity*

3.7 Machine Learning Algorithms

In the first phase, the planner begins by preparing the data, including reading the data from the Excel file, splitting features and targets, splitting data for training, testing ML algorithms, and scaling features. The data set is being read from the selected Excel file, where the data is obtained from sensors' measurements. The leading or trailing white space is removed from the column names. The input features and the target variable are separated from the data table in Excel. The data set is divided into training and testing using the train_test_split function from the scikit-learn library. Next, scale features normalize input features using a standard scaler from the scikit-learn library.

The ML models, including SVM, RF, DT, and KNN, are developed in the second phase. Following this, the ML models are trained using a training dataset. The output file obtained from the training process is stored on the computer. The tested dataset evaluates the ML models in the third phase. Performance metrics, such as accuracy, precision, recall, F1 score, AUC, and specificity, are computed based on confusion matrix parameters. The program then gives the outcomes of the calculated performance metrics; if the accuracy is high, it moves to the next step; otherwise, it retests the data.

In the fourth phase, the user interface is designed to predict the DFU based on entered values. Design the GUI: The Tkinter interface starts with titles and labels for input features, as shown in Figs. 10(a) and 10(b). Includes text input fields, allowing users to enter values for each of the twelve features. Once the user enters the physiological features into the fields shown in the Tkinter GUI (right side of Figs. 10(a) and 10(b)), the user can click on the "Predict" button to obtain the status of the DFU as healthy or unhealthy. The performance metrics are displayed on the left side of Fig. 10(a) and 10(b).

Machine learning algorithms require careful tuning of hyperparameters to enhance performance and prevent overfitting or poor generalization. For DT, it is recommended to set max_depth between 5 and 10, min_samples_split between 2 and 10, min_samples_leaf between 1 and 4, and select criterion as "gini" or "entropy". For RF, hyperparameters include n_estimators from 100 to 500, max_depth from 5 to 15, min_samples_split between 2 and 10, min_samples_leaf between 1 and 4, and max_features as "sqrt" or "log2". In KNN, it is recommended to set n_neighbors between 3 and 15, choose weights as "uniform" or "distance", and metric as "minkowski" with p=2. For SVM, important hyperparameters include kernel as "linear" or "rbf", C from 0.1 to 10, gamma as "scale" or "auto", and probability=True if probabilistic predictions are required.

Int. Journal of Integrated Engineering Vol. 18 No. 3 (2026) p. 366-388

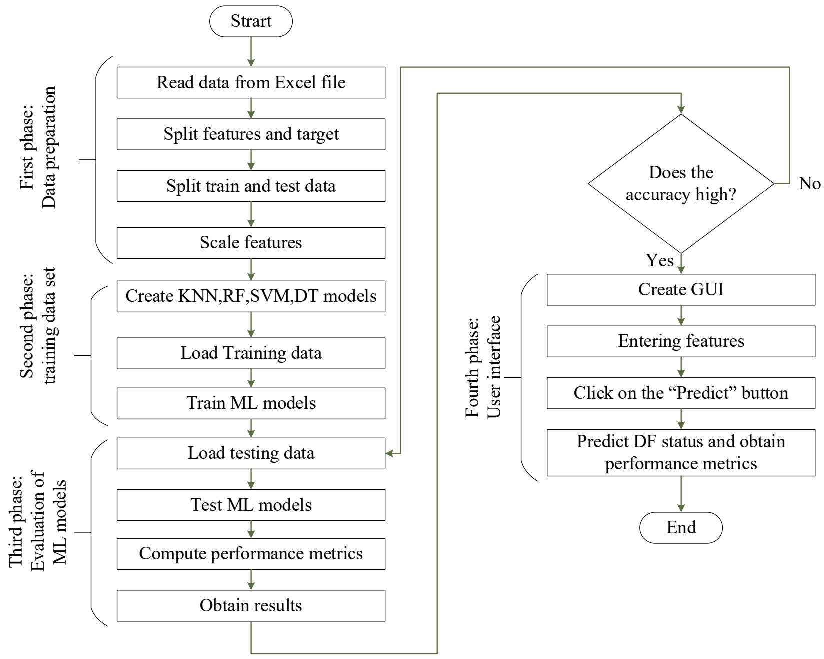

Fig. 9 *Flowchart of the ML algorithm*

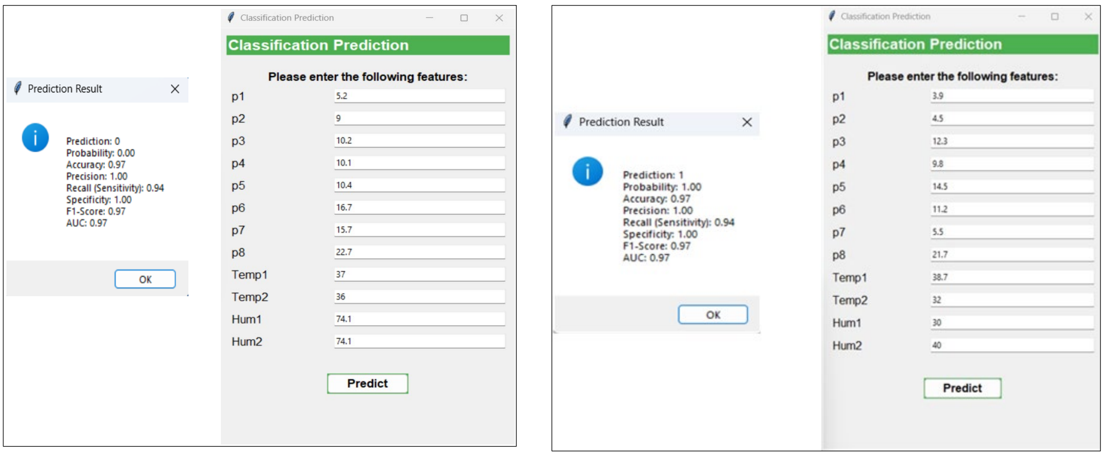

(a) **(b)**

Fig. 10 *User interface for entering physiological data to predict DFU (a) A healthy foot; and (b) An unhealthy foot*

3.8 System Evaluation

Performance metrics are vital criteria for evaluating ML models. These metrics include several key aspects, starting with accuracy, representing the ratio of correct predictions to total predictions, represented by Equation (5) [46, 47]. It is also worth highlighting specificity, which measures the model's ability to recognize true negatives and is referred to as Equation (6) [48, 49]. To attain an overall evaluation, the F1-score is used, which calculates the harmonic mean between precision and recall, as shown in Equation (7) [50].

Furthermore, the AUC is used to evaluate the model's ability to discriminate between classes, according to Equation (8) [51]. Recall is a metric that quantifies the proportion of true positives accurately recognized by the model, as shown by Equation (9) [52]. Finally, precision is used to evaluate the accuracy in classifying positive patterns. This is the ratio of correctly classified positive shapes to the total number of positive shapes classified. Calculate it using a specific formula (10) [53]. These metrics are widely adopted to evaluate models and determine their efficiency in classifying data and predicting outcomes. Most of these equations are based on specifying true positive (TP), false positive (FP), true negative (TN), and false negative (FN) parameters. Each parameter is defined as follows.

- TP: The number of cases in which the model correctly predicted a positive outcome [54].
- FP: The number of cases in which the model predicted a positive outcome, but the actual outcome was negative [55].

- TN: The number of cases in which the model correctly predicted a negative outcome [56].
- FN: The number of cases in which the model predicted a negative outcome, but the actual outcome was positive [57].

$$Accuracy\ (Acc) = \frac{TP + TN}{TP + TN + FN + FP} \quad (5)$$

$$Specificity\ (Spe) = \frac{TN}{TN + FP} \quad (6)$$

$$F1 - Score\ (F1 - Sco) = 2 \times \frac{Pre * Rec}{Prec + Rec} \quad (7)$$

$$AUC = \int_0^1 TPR(t)\,dt \quad (8)$$

$$Recall\ (Rec) = \frac{TP}{TP + FN} \quad (9)$$

$$Precision\ (Pre) = \frac{TP}{TP+FP} \quad (10)$$

4. Results and Discussion

This section presents the results of the ML algorithms used in this research based on physiological data from the foot. It shows their performance based on different performance metrics and confusion matrices to identify the best performers. Confusion matrices compare the model predictions to the actual data. As explained in Section 3.6, these matrices typically consist of four entries: TP, TN, FP, and FN, and are necessary to calculate performance metrics such as accuracy, recall, specificity, AUC, F1 scores, and precision. Analysis of the confusion matrices of the models provides important information about the classification accuracy. This information is essential to understand each model's strengths and weaknesses and identify the best model for the given task. Fig. 11 presents the confusion matrices of the four supported ML algorithms: SVM, KNN, RRF, and DT.

As can be seen in the first confusion matrix of the SVM model (Fig. 11(a)), the model had 29 TN and 29 TP, indicating that the model can assign both correct negative and correct positive cases. Nevertheless, it had 4 FP where the model falsely identified positive when the true class was negative and 6 FN, where the model could not identify the positive cases. It means that the performance was rather balanced, but with a significant amount of misclassifications on both ends.

The second confusion matrix of KNN (Fig. 11(b)) yields a better result than that of SVM. In this case, the model rightly categorized 32 TN and 33 TP, and fewer incidents of misclassification, 2 FP and 3 FN. This is an indicator of greater correct detection of the two classes and indicates improved overall recall and precision. The fact that the number of mistakes has been minimized shows that the model has become more effective when it comes to determining the differences between the two categories.

The performance is then even better in the third confusion matrix of RF (Fig. 11(C)) since the model did not have any false positives (FP = 0) at all, implying that it did not point towards a negative case as a positive one. It had a correct prediction of 34 TN and 33 TP, with 3 FN remaining. It means that the precision is very high because all the positive predictions of the model have been correct. Nevertheless, the false negatives indicate the existence of a few false positives, which has an impact on sensitivity a little.

Fig. 11(d) is the fourth confusion matrix of RF, and it has the best performance. In the model, the values were 32 TN and 36 TP, and 0 FP and 1 FN. This is a great precision because almost everything was rightly identified, and the mistakes were few. The high precision is guaranteed by the fact that there are no false positives, and the false negatives are extremely low, which shows that the recall is high. Overall, this setting demonstrates that the model has obtained almost optimal classification power.

These results imply that the incorrect diagnosis of mild DFU as normal might delay early intervention, and the correct diagnosis of severe DFU provides prompt medical intervention.

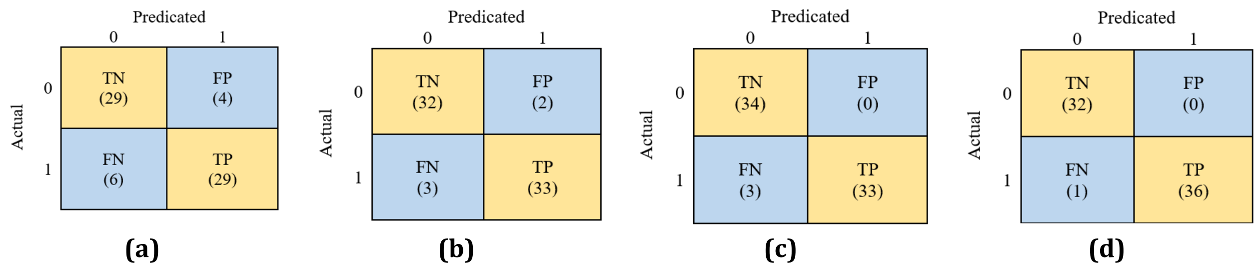

Fig. 11 *Confusion matrices for the adopted algorithms: (a) SVM; (b) KNN; (c) RF; and (d) DT; showing correct classifications on the diagonal and misclassifications off-diagonal*

Table 4 shows the performance characteristics of four ML algorithms: SVM, KNN, RF, and DT. The SVM achieves impressive results overall, with an accuracy of 83%, indicating its exceptional ability to accurately predict positive and negative outcomes. KNN performs well with an accuracy of 93%, demonstrating reliability in predicting positive and negative outcomes. RF obtained an accuracy of 96%, indicating strong classification performance. DT showed the highest performance among the presented algorithms, with an accuracy of 99%, indicating its excellent ability to discriminate between classes. The F1 rate is significant because it balances accuracy and is particularly useful in cases where the cost of positive and negative errors is equal. Specificity and recall are also essential to evaluate the model's ability to predict negative and positive cases correctly. Overall, the results show that the algorithms used provide high performance. However, results depend on the data and the specific task the models are trained to perform. It is also essential to consider the balance between classes in the data to avoid prediction bias.

Table 4 *Performance metrics for different ML algorithms*

ML	Acc (%)	AUC (%)	F1-Sco (%)	Spe (%)	Rec (%)	Pre (%)
SVM	85	95	85	88	83	88
KNN	93	99	93	94	92	94
RF	96	99	96	100	92	100
DT	99	99	99	100	97	100

DT performs well and shows high performance and superiority due to the following reasons (i) DT handles small and heterogeneous datasets effectively, which suits our dataset that combines different sensor types, (ii) DT can process continuous features (e.g., pressure, temperature) and categorical outcomes without requiring extensive normalization, (iii) DT provides transparent decision-making rules, which is critical in medical applications where explainability is essential. These characteristics make DT more robust and reliable in DFU prediction compared to the other tested algorithms.

Fig. 12 shows the evaluation of the DT model for the Receiver Operating Characteristic (ROC) curve, precision-recall curve, and learning curve. Fig. 12(a) shows the ROC curve, which is a graphical representation technique to measure the performance of any binary classification model. In ROC, the generated curves compare the True Positive Rate (sensitivity) on the y-axis with the False Positive Rate (specificity) ratio on the x-axis under different threshold settings. The diagonal dashed line is a performance of a random classifier, where the true positive rate is the same as the false positive rate, and acts as a plane. The overall discrimination between classes keeps the entire value of the ROC curve, i.e., the area under the ROC curve (AUC). As the figure shows, the ROC curve is almost at the top of the right corner of the plot, which is a sign of a high true and a low false positive rate for most of the thresholds. The AUC value of 0.97 indicates that the model has a high discriminating rule because an AUC of 1.0 is the exact classification, and 0.5 is a random guess. The model under consideration also shows extremely good results in differentiating the two classes, which is proven by the large value of the AUC indicator and the structure of the ROC curve.

Fig. 12(b) indicates a Precision-Recall (PR) plot that enables one to analyze the performance of a binary discrimination design, particularly when lop-sided data is used. The PR curve is a curve where precision (proportion of the right positive predictions of the model to the total number of positive predictions) is on the y-axis and recall (proportion of true positives recognized by the model to the total number of actual positives) is on the x-axis. In contrast to the ROC curve, the PR curve concentrates on the performance regarding the positive class, which makes this curve especially beneficial in the case of the rare or sensational positive category. The outcomes in the figure show that the model obtains very high precision and recall values within the majority of the threshold range. Precision is close to 1.0 in almost all recall values, except towards the end, where recall approaches 1.0. This implies that the model can distinguish as close as possible all positive cases with very few false alarms. The drop at the end is characteristic as the threshold becomes so low that the model predicts almost all the cases to be positive, which triggers the recall to be the maximum at the expense of the decrease in precision. Overall, this PR curve proves that the model performs well, successfully balancing precision and recall with most thresholds.

Fig. 12(c) shows a learning curve, a diagnostic device in machine learning to examine the alteration in the performance of a model as the training data size improves. The x-axis is the training size (or the number of training sizes): the y-axis is the accuracy, the percentage of correct predictive answers. The figure shows two curves: the first is the blue line that represents the training score, which indicates how well the model performs on the training data, and the orange one that represents the cross-validation score, which shows the model's performance on newly generated validation data. The training score initially begins very high (approximating 1.0), and as the size of the training goes up, the training score decreases since the model fits the small training dataset poorly. Nevertheless, the training accuracy slightly drops as the amount of data is increased, as it is expected that the model needs to generalize over a larger and more heterogeneous dataset. The training score is highly consistent and indicates that the model does not have major trouble fitting the training data, regardless of the increase in the dataset size.

However, the cross-validation score is initially a lot lower than the training score when the size is small. Such a gap is normal since with not much data, the model will overfit, i.e., perform well on the training set but perform very worse on the unseen data. The accuracy of cross-validation improves significantly as the training size rises, indicating that the model generalizes well, and the more data sizes used to train the model. The cross-validation curve keeps rising afterward and then begins to level off, which means that the advantages of including more data decrease, and the model's generalization performance eventually becomes steady. The findings show that the model responds well to more training data, increasing cross-validation accuracy significantly. The fact that the difference between the training and cross-validation scores tends to decrease with the increase in the training size indicates that one is minimizing overfitting. Because the two scores converge at a high rate of accuracy then this implies that the model is not only accurate but is also general, and implies that the learning is well balanced and effective. Such a learning curve would indicate a good performance of the model and a healthy training regime, and there is not much evidence of high bias or high variance issues.

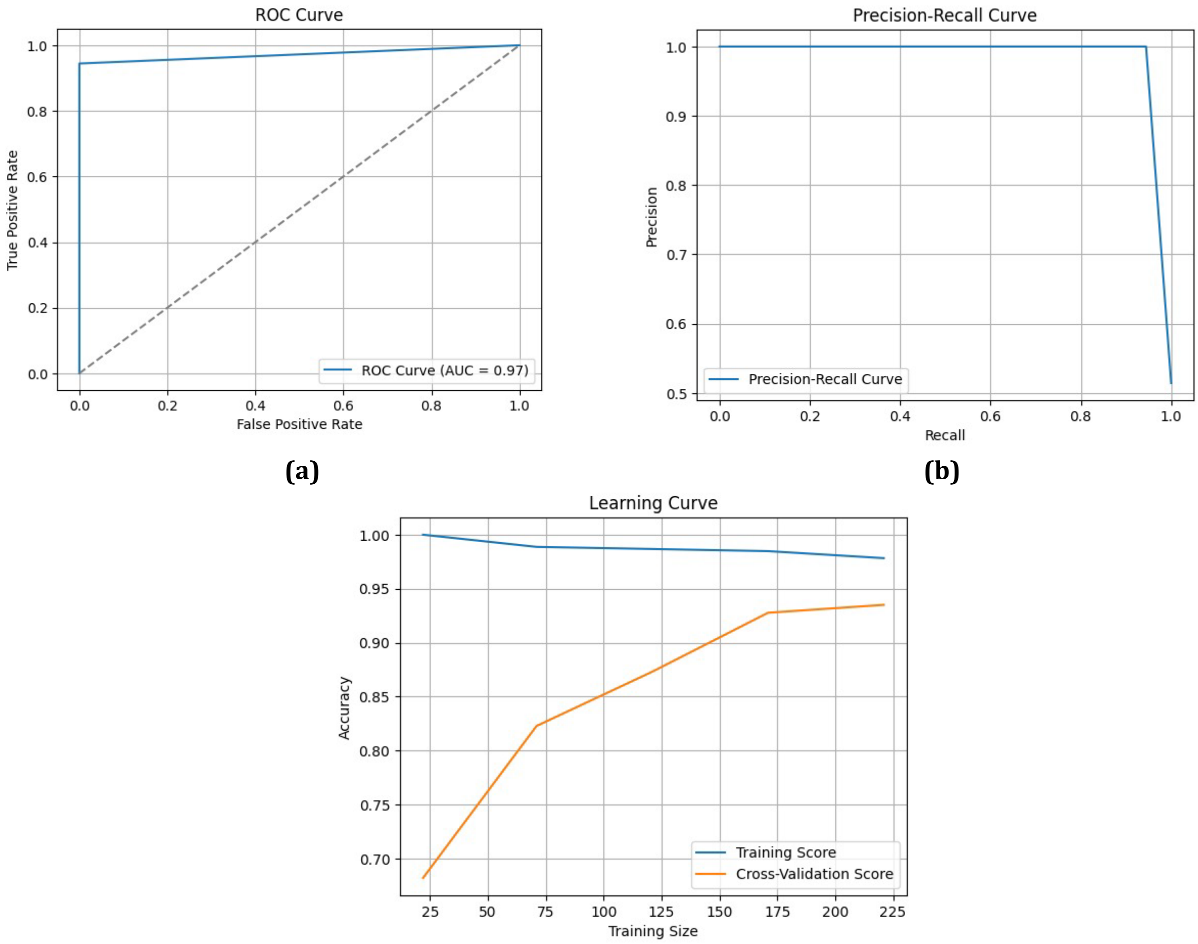

(a) (b)

(c)

Fig. 12 *Graphs evaluation of the DT model (a) ROC curve; (b) Precision-recall curve; (c) Learning curve*

Int. Journal of Integrated Engineering Vol. 18 No. 3 (2026) p. 366-388

5. Results Comparison

The results in this study can be evaluated through accuracy, recall, specificity, AUC, F1-score, and precision to confirm the effectiveness of our approach by comparing it against previous works. This comparison verifies the robustness and reliability of the suggested models and emphasizes their advancements over existing solutions, confirming their potential for real-world clinical uses in DFU diagnosis. Table 5 compares our results with those from previous studies.

Our method appears in Table 5 alongside previous research to examine both subject numbers and the utilization of AI methods. The referenced works use different machine learning techniques, including DT, SVM, RF, MLPNN, and deep learning models, such as EfficientNet and Inception-ResNetV2. The DT-based approach for patient classification utilizes 300 subjects' physiological information to establish a strong AI implementation model. The limited number of subjects in Radunovic et al.'s study [32], with 23 participants, reduced the external validity of their research findings. The research of Haque et al. [28] uses various ML models with a small dataset (i.e., 45 participants) that reduces the trustworthiness of their research findings. The performance metrics of our approach surpass most previous studies by reaching 99% accuracy alongside 100% specificity, 99% F1-score, 99% AUC, 97% recall, and 100% precision. The research conducted by Wang et al. [26] resulted in 94.7% accuracy, while Chauhan et al. [27] obtained 94.0% accuracy through different research methods and data limitations. The classification capabilities of DT surpass those exhibited by Ferreira et al.'s [29] MLPNN-based approach since the latter only achieved 85% accuracy. Our work shows superior consistency in key performance indicators compared to Basiri et al. [30] (EfficientNet) because of its ability to handle dataset imbalance issues.

Previous research methods, which led to inaccurate classification results, have encountered various issues. The researchers Cassidy et al. [31] and Radunovic et al. [32] experienced time limitations and sensor stability issues that might have influenced their study results. Two studies by Haque et al. [28], together with Ferreira et al. [29], faced difficulties due to sparse datasets, thus reducing the applicability of their experimental results. Gudivaka et al. [36] needed advanced hardware infrastructure and did not apply sufficient model optimization, which made their program difficult to implement. Our methodology utilizes an AI model that works with a balanced set of research data to avoid the limitations described in other studies. Our study's research outcomes fall behind Fadhel et al.'s work [34] (2024), which used DFU_TFNet and DFU_FNet models to reach 99.81% accuracy and 99.76% recall. The better results achieved by their approach stem from employing advanced deep learning models that utilize VGG-16, GoogleNet, and AlexNet to extract features having high discrimination capabilities. The proposed method encounters two main limitations: high memory requirements and extra steps to distinguish varied DFU types. Our DT-based model achieves high performance alongside computational efficiency, which makes it more applicable to practical implementations. The performance gap can be reduced by implementing ensemble learning and additional feature engineering as potential upgrades to the system.

Table 5 *Comparison results with previous works*

Ref. /Year	AI	Acc (%)	Spe (%)	F1-Sco (%)	AUC (%)	Rec (%)	Pre (%)	Data used (subject/ image)	Limitations (Categorized)
Wang et al. [26]/ 2021	RF	94.7	N/A	N/A	N/A	N/A	N/A	2,403	**Validation gap:** Not suitable for continuous observation in daily life, limiting practical DFU risk assessment.
Chauhan et al. [27] / 2023	KNN SVM	94.0	N/A	93.1	N/A	93.4	92.7	110	**Validation gap:** Generalizability is limited due to specific ML algorithms/features.
Haque et al. [28] / 2022	DAC, ECM, KCM, KNN, LCM, NBC, SVM, BDC	98.68	N/A	98.68	1.00	98.68	98.72	45	**Dataset size:** Very small dataset (3 groups only). **Validation gap:** Requires larger and more diverse datasets for generalization.
Ferreira et al. [29] /2023	MLPNN	85	91	N/A	N/A	76	89	250	**Dataset size:** Data collected from a single institution only limited generalizability.
Basiri et al. [30] / 2024	EfficientNet	N/A	N/A	79	N/A	74	86	269	**Validation gap:** Imbalanced training dataset not addressed → risk of biased results.
Cassidy et al. [31] /2023	R-CNN, Inception-ResNetV2	92.12	91.67	94.8	N/A	92.26	97.48	81	**Validation gap:** Short study period (Sept 2020–Jan 2021) → no long-term validation.
Radunovic et al. [32] / 2024	SVM, DT, LR	82.1	87	82.88	N/A	78	88.46	23	**Hardware issue:** Sensor/application technical problems → unreliable results.
Salih et al. [33]/ 2024	SVM, RF, DT, Naïve Bayes	89.86	N/A	89.91	93.72	89.77	89.18	768	**Validation gap:** Lack of multidimensional data → low diagnostic accuracy.
Fadhel et al. [34]/2024	DFU_TFNet, DFU_FNet, VGG-16, GoogleNet, AlexNet.	99.81	N/A	99.25	N/A	99.76	99.38	754	**Hardware issue:** High memory requirement. **Validation gap:** Missing vital features. **Sensor stability:** Extra layers reduce performance stability.
Rathore et al. [35]/2025	Xception, DenseNet121, ResNet50, InceptionV3, MobileNetV2, SNN	98.76	99.2	98.5	98.6	97.7	99.3	1,050	**Validation gap:** Limited adaptability to other conditions/datasets. **Hardware issue:** Real-world implementation challenges. **Dataset size:** Limited dataset boundaries restrict generalization.
Gudivaka et al. [36]/2025	SVM, ELM, AlexNet, VGG16, GoogLeNet, ResNet50	93.75	81.03	84.09	N/A	86.93	81.43	385	**Hardware issue:** High computational cost. **Validation gap:** Lack of hyperparameter tuning details. **Sensor stability:** Complex method difficult for clinicians to interpret.
This work/ 2025	**DT**	**99**	**100**	**99**	**99**	**97**	**100**	**300 patients' physiological data**	**Dataset size: Limited DFU volunteers. Hardware issue: Sensor accuracy challenges.**

DAC: Discriminant analysis classifier; ECM: Ensemble classification model; KCM: Kernel classification model; LCM: Linear classification model; NBC: Naive Bayes classifier; BDC: Binary decision classification tree; R-CNN: Region-based Convolutional Neural Network; LR: logistic regression; SNN: Siamese Neural Network; ELM: Extreme Learning Machines

6. Conclusions

DFU complications can be severe complications and may lead to amputation of limbs. Therefore, early detection of this disease is essential to avoid such complications. Screening methods for the disease can be conventional and do not predict DFU in the early stages. These prompted researchers to find an alternative WSN solution to detect DFU early. ML algorithms using data processing and feature extraction techniques have shown outstanding performance in healthcare applications. However, depending on the desired application, some may perform better. This proposed study achieved a performance comparison between four standard ML algorithms that used physiological data. The DT algorithm achieved the best results with 99% accuracy in classifying the two categories. At the same time, SVM showed the lowest performance, with 85% accuracy. However, the current study faced two limitations: difficulty in obtaining a larger number of DFU patient volunteers and challenges in sensors accuracy. These limitations will be addressed in future work by collaborating with multiple hospitals to expand the dataset, employing data augmentation techniques to mitigate small sample size issues, and improving sensor robustness.

Furthermore, future applications of our system may include home-based monitoring kits for diabetic patients to check their foot health daily and clinic-based screening tools to support physicians in early DFU detection. Such applications will enhance the real-world impact by reducing late diagnoses and lowering the risk of foot amputations.

Acknowledgements

The authors thank the Department of Medical Instrumentation Engineering Techniques faculty at the Electrical Engineering Technical College, Middle Technical University-Baghdad, Iraq, for cooperating.

Conflict of interest

The authors have no competing interests to declare relevant to this article's content.

Author contribution

The authors confirm contribution to the paper as follows: ***Conceptualization:*** *Sadik Kamel Gharghan, Ahmed Akeel Ali, and Adnan Hussein Ali;* ***Methodology:*** *Sadik Kamel Gharghan, Ahmed Akeel Ali, and Adnan Hussein Ali;* ***Formal analysis and investigation:*** *Sadik Kamel Gharghan and Ahmed Akeel Ali;* ***Writing - original draft preparation:*** *Ahmed Akeel Ali;* ***Writing - review and editing:*** *Sadik Kamel Gharghan and Adnan Hussein Ali;* ***Resources:*** *Ahmed Akeel Ali;* ***Supervision:*** *Adnan Hussein Ali.*

References

[1] Xuefei Zhao, Xuedong An, Cunqing Yang, Wenjie Sun, Hangyu Ji, and Fengmei Lian (2023). The crucial role and mechanism of insulin resistance in metabolic disease. *Frontiers in endocrinology, 14*, 1149239, doi: https://doi.org/10.3389/fendo.2023.1149239.

[2] Yeo Kwon Yoon, Jae Han Park, Hang Hwan Cho, Dong Woo Shim, Wonwoo Lee, Seung Hwan Han, Jin Woo Lee, and Kwang Hwan Park (2025). Red blood cell distribution width is an independent predictor of mortality following amputation for diabetic foot. *Scientific Reports, 15(1)*, 4441, doi: 10.1038/s41598-025-85684-x.

[3] Padmalaya Nayak, J. Siva Naga Jyothi, V. Harika, K. Swaraja, and A. Sai Hanuman (2025). Diabetes Monitoring and Prediction Using Computational Intelligence Techniques: A Systematic Review. *SN Computer Science, 6(3)*, 267, doi: 10.1007/s42979-025-03802-y.

[4] Andrew JM Boulton (2019). The diabetic foot. *Medicine, 47(2)*, 100-105, doi: https://doi.org/10.1016/j.mpmed.2018.11.001.

[5] Arokia Vijaya Anand Mariadoss, Allur Subramaniyan Sivakumar, Chang-Hun Lee, and Sung Jae Kim (2022). Diabetes mellitus and diabetic foot ulcer: Etiology, biochemical and molecular based treatment strategies via gene and nanotherapy. *Biomedicine & Pharmacotherapy, 151*, 113134, doi: https://doi.org/10.1016/j.biopha.2022.113134.

[6] Sandra Sif Gylfadottir, Danita Weeracharoenkul, Signe Toft Andersen, Supranee Niruthisard, Sompongse Suwanwalaikorn, and Troels Staehelin Jensen (2019). Painful and non-painful diabetic polyneuropathy: clinical characteristics and diagnostic issues. *Journal of diabetes investigation, 10(5)*, 1148-1157, doi: https://doi.org/10.1111/jdi.13105.

[7] Chiara Lauri, Antonio Leone, Marco Cavallini, Alberto Signore, Laura Giurato, and Luigi Uccioli (2020). Diabetic foot infections: the diagnostic challenges. *Journal of clinical medicine, 9(6)*, 1779, doi: https://doi.org/10.3390/jcm9061779.

[8] Maria Nikoloudi, Ioanna Eleftheriadou, Anastasios Tentolouris, Ourania A Kosta, and Nikolaos Tentolouris (2018). Diabetic foot infections: update on management. Current infectious disease reports, 20, 1-11, doi: https://doi.org/10.1007/s11908-018-0645-6.

[9] Aparna Komarraju and Avneesh Chhabra (2020). Advanced Cross-Sectional Radiology-Ultrasound, Computed Tomography and Magnetic Resonance Imaging of the Diabetic Foot. The Foot in Diabetes, 169-185, doi: https://doi.org/10.1002/9781119445821.ch10.

[10] Kirubel Eshetu Haile, Yordanos Sisay Asgedom, Gedion Asnake Azeze, Atitegeb Alebachew Amsalu, Amanuel Yosef Gebrekidan, and Gizachew Ambaw Kassie (2025). Diabetic foot: A systematic review and meta-analysis on its prevalence and associated factors among patients with diabetes mellitus in a sub-Saharan Africa. *Diabetes Research and Clinical Practice, 220*, 111975, doi: https://doi.org/10.1016/j.diabres.2024.111975.

[11] Federica Verdini, Alessandro Mengarelli, Gaetano Chemello, Benedetta Salvatori, Micaela Morettini, Christian Göbl, and Andrea Tura (2025). Sensors and Devices Based on Electrochemical Skin Conductance and Bioimpedance Measurements for the Screening of Diabetic Foot Syndrome: Review and Meta-Analysis. *Biosensors, 15(2)*, 73, doi: https://doi.org/10.3390/bios15020073.

[12] David Reifs Jiménez, Lorena Casanova-Lozano, Sergi Grau-Carrión, and Ramon Reig-Bolaño (2025). Artificial Intelligence Methods for Diagnostic and Decision-Making Assistance in Chronic Wounds: A Systematic Review. *Journal of Medical Systems, 49(1)*, 29, doi: 10.1007/s10916-025-02153-8.

[13] Siraj Qays Mahdi, Sadik Kamel Gharghan, and Muhideen Abbas Hasan (2021). FPGA-Based neural network for accurate distance estimation of elderly falls using WSN in an indoor environment. *Measurement, 167*, 108276, doi: https://doi.org/10.1016/j.measurement.2020.108276.

[14] Sadik K. Gharghan, Rosdiadee Nordin, and Mahamod Ismail (2015). An Ultra-Low Power Wireless Sensor Network for Bicycle Torque Performance Measurements. *Sensors, 15(5)*, 11741-11768, doi: https://doi.org/10.3390/s150511741.

[15] HaoRan Tao, Lili You, Yuhan Huang, Yunxiang Chen, Li Yan, Dan Liu, Shan Xiao, Bichai Yuan, and Meng Ren An interpreting machine learning models to predict amputation risk in patients with diabetic foot ulcers: a multi-center study. *Frontiers in Endocrinology, 16*, 1526098, doi: https://doi.org/10.3389/fendo.2025.1526098.

[16] Shichai Hong, Yihui Chen, Yue Lin, Xinsheng Xie, Gang Chen, Hefu Xie, and Weifeng Lu (2024). Personalized prediction of diabetic foot ulcer recurrence in elderly individuals using machine learning paradigms. *Technology and Health Care, 32(1_suppl)*, 265-276, doi: https://doi.org/10.3233/THC-248023.

[17] Ge Shi, Zhenxuan Gao, Ze Zhang, Quanyu Jin, Sitong Li, Jiaxin Liu, Lei Kou, Abudurezhake Aerman, Wenqiang Yang, and Qi Wang (2025). Machine learning-based risk prediction model for neuropathic foot ulcers in patients with diabetic peripheral neuropathy. *Journal of Diabetes Investigation*, doi: https://doi.org/10.1111/jdi.70010.

[18] Teruji Ide (2024). An Evaluation on EMG-based Machine Learning Classification of Hand Movements Using Three Electrodes Arrangement on Forearm. *International Journal of Integrated Engineering, 16(9)*, 398-409, doi: https://doi.org/10.30880/ijie.2024.16.09.032.

[19] Rachita Nanda, Abhigyan Nath, Suprava Patel, and Eli Mohapatra (2022). Machine learning algorithm to evaluate risk factors of diabetic foot ulcers and its severity. *Medical & Biological Engineering & Computing, 60(8)*, 2349-2357, doi: 10.1007/s11517-022-02617-w.

[20] Anna A. Poradzka and Leszek Czupryniak (2023). The use of the artificial neural network for three-month prognosis in diabetic foot syndrome. *Journal of Diabetes and its Complications, 37(2)*, 108392, doi: https://doi.org/10.1016/j.jdiacomp.2022.108392.

[21] Khadraa Mohamed Mousa, Farid Ali Mousa, Helalia Shalabi Mohamed, and Manal Mohamed Elsawy (2023). Prediction of foot ulcers using artificial intelligence for diabetic patients at Cairo university hospital, Egypt. *SAGE open nursing, 9*, 23779608231185873, doi: https://doi.org/10.1177/23779608231185873.

[22] Zhilu Ye, Xinran Li, Kun Zhao, Wang Zhan, Qi Zhang, Lei Lei, Minye Yang, Ming Liu, and Xiaohui Zhang (2025). Sensitive and reliable wireless monitoring of foot pressure and temperature for diabetic foot ulcer management and prevention. *Sensors and Actuators A: Physical, 387*, 116411, doi: https://doi.org/10.1016/j.sna.2025.116411.

[23] Malik Adnan, Junaid Saddiqi, Muhammad Hamza Zulfiqar, Muhammad Atif Khan, Khaled Al-Jaloud, Ali H. Alqahtani, Rifaqat Hussain, and Muhammad Qasim Mehmood (2025). IDC Pressure Sensors Enabled Smart Footwear System for In Vitro Detection and Monitoring of Diabetic Foot Ulcer. *Sensors and Actuators A: Physical*, 116489, doi: https://doi.org/10.1016/j.sna.2025.116489.

[24] Mohammed Abdulla Salim Al Husaini, Mohamed Hadi Habaebi, Teddy Surya Gunawan, and Md Rafiqul Islam (2021). Self-detection of early breast cancer application with infrared camera and deep learning. *Electronics, 10(20)*, 2538, doi: https://doi.org/10.3390/electronics10202538.

[25] Rui Hong, Chenglang Xiang, Hui Liu, Adam Glowacz, and Wei Pan (2019). Visualizing the knowledge structure and research evolution of infrared detection technology studies. *Information, 10(7)*, 227, doi: https://doi.org/10.3390/info10070227.

[26] D. Wang, J. Ouyang, P. Zhou, J. Yan, L. Shu, and X. Xu (2021). A Novel Low-Cost Wireless Footwear System for Monitoring Diabetic Foot Patients. *IEEE Trans Biomed Circuits Syst, 15(1)*, 43-54, doi: 10.1109/TBCAS.2020.3043538.

[27] A. S. Chauhan, M. S.Varre, K. Izuora, M. B. Trabia, and J. S. Dufek (2023). Prediction of Diabetes Mellitus Progression Using Supervised Machine Learning. *Sensors, 23(10)*, doi: 10.3390/s23104658.

[28] F. Haque, M. B. I.Reaz, M. E. H.Chowdhury, M. Ezeddin, S. Kiranyaz, M. Alhatou, S. H. M. Ali, A. A. A. Bakar, and G. Srivastava (2022). Machine Learning-Based Diabetic Neuropathy and Previous Foot Ulceration Patients Detection Using Electromyography and Ground Reaction Forces during Gait. *Sensors, 22(9)*, doi: 10.3390/s22093507.

[29] Acbh Ferreira, D. D. Ferreira, B. H. G. Barbosa, U. Aline de Oliveira, E. Aparecida Padua, F. Oliveira Chiarini, and M. H. Baena de Moraes Lopes (2023). Neural network-based method to stratify people at risk for developing diabetic foot: A support system for health professionals. *PLoS One, 18(7)*, e0288466, doi: 10.1371/journal.pone.0288466.

[30] R. Basiri, K. Manji, P. M. LeLievre, J. Toole, F. Kim, S. S. Khan, and M. R. Popovic (2024). Protocol for metadata and image collection at diabetic foot ulcer clinics: enabling research in wound analytics and deep learning. *Biomed Eng Online, 23(1)*, 12, doi: 10.1186/s12938-024-01210-6.

[31] B. Cassidy, M. Hoon Yap, J. M. Pappachan, N. Ahmad, S. Haycocks, C. O'Shea, C. J. Fernandez, E. Chacko, K. Jacob, and N. D. Reeves (2023). Artificial intelligence for automated detection of diabetic foot ulcers: A real-world proof-of-concept clinical evaluation. *Diabetes Res Clin Pract, 205*, 110951, doi: 10.1016/j.diabres.2023.110951.

[32] G. Radunovic, Z. Velickovic, S. Pavlov-Dolijanovic, S. Janjic, B. Stojic, I. Jeftovic Velkova, N. Suljagic, and I. Soldatovic (2024). Wearable Movement Exploration Device with Machine Learning Algorithm for Screening and Tracking Diabetic Neuropathy-A Cross-Sectional, Diagnostic, Comparative Study. *Biosensors, 14(4)*, doi: 10.3390/bios14040166.

[33] Merdin Shamal Salih, Rowaida Khalil Ibrahim, SR Zeebaree, Dilovan Asaad, Lozan M Zebari, and Nasiba Mahdi Abdulkareem (2024). Diabetic prediction based on machine learning using PIMA indian dataset. *Communications on Applied Nonlinear Analysis, 31(5s)*, 138-156.

[34] Mohammed A. Fadhel, Laith Alzubaidi, Yuantong Gu, Jose Santamaría, and Ye Duan (2024). Real-time diabetic foot ulcer classification based on deep learning & parallel hardware computational tools. *Multimedia Tools and Applications, 83(27)*, 70369-70394, doi: 10.1007/s11042-024-18304-x.

[35] Pramod Singh Rathore, Abhishek Kumar, Amita Nandal, Arvind Dhaka, and Arpit Kumar Sharma (2025). A feature explainability-based deep learning technique for diabetic foot ulcer identification. *Scientific Reports, 15(1)*, 6758, doi: 10.1038/s41598-025-90780-z.

[36] Raj Kumar Gudivaka, Rajya Lakshmi Gudivaka, Basava Ramanjaneyulu Gudivaka, Dinesh Kumar Reddy Basani, Sri Harsha Grandhi, and Faheem khan (2025). Diabetic foot ulcer classification assessment employing an improved machine learning algorithm. *Technology and Health Care*, 09287329241296417, doi: https://doi.org/10.1177/09287329241296417.

[37] Jahedul Islam, Umme Habiba, Humayun Kabir, Kazi Golam Martuza, Fahmida Akter, Farhana Hafiz, Mohammod Abu Sayid Haque, Mahbubul Hoq, and Md A Mannan (2018). Design and development of microcontroller based wireless humidity monitor. *IOSR Journal of Electrical and Electronics Engineering, 13(2)*, 41-46, doi: 10.9790/1676-1302034146

[38] Petr Foltýnek, Marek Babiuch, and Pavel Šuránek (2019). Measurement and data processing from Internet of Things modules by dual-core application using ESP32 board. *Measurement Control, 52(7-8)*, 970-984, doi: https://doi.org/10.1177/0020294019857748.

[39] George Constantin, Iosif-Adrian Maroșan, Mihai Crenganiș, Corina Botez, Claudia-Emilia Gîrjob, Cristina-Maria Biriș, Anca-Lucia Chicea, and Alexandru Bârsan (2023). Monitoring the Current Provided by a Hall Sensor Integrated in a Drive Wheel Module of a Mobile Robot. *Machines, 11(3)*, 385, doi: https://doi.org/10.3390/machines11030385.

[40] Wan Nur Suryani Firuz Wan Ariffin, Cheah Seng Keat, Terrance Prasath, Ludhaya Suriyan, Nurfadzilah Aqilah Mohamad Nore, Nur Baya Mohd Hashim, and Aini Syuhada Md Zain, "Real-time dynamic traffic light controlsystem with emergency vehicle priority," *in Journal of Physics: Conference Series*, 2021, vol. 1878, no. 1: IOP Publishing, p. 012063.

[41] Manuel Jesús Espinosa-Gavira, Agustín Agüera-Pérez, José María Sierra-Fernández, Juan José González de-la-Rosa, José Carlos Palomares-Salas, and Olivia Florencias-Oliveros (2022). Design and Test of a High-Performance Wireless Sensor Network for Irradiance Monitoring. *Sensors, 22(8)*, 2928, doi: https://doi.org/10.3390/s22082928.

[42] Abdel-Nasser Sharkawy, Mahmoud Hasanin, Mohamed Sharf, Mahmoud Mohamed, and Ahmed Elsheikh (2022). Development of smart home applications based on arduino and android platforms: an experimental work. *Automation in Construction, 3(4)*, 579-595, doi: https://doi.org/10.3390/automation3040029.

[43] Bharath Kumar Komatineni, Sangram Kishore Satpathy, Mude Arjunb Naik, Utkarsh Dwivedi, and Jyoti Lahre (2024). An unmanned rice seeder with WiFi based mobile-control system for drudgery reduction. *Smart Agricultural Technology, 8*, 100471, doi: https://doi.org/10.1016/j.atech.2024.100471.

[44] Ignas Plauska, Agnius Liutkevičius, and Audronė Janavičiūtė (2022). Performance evaluation of c/c++, micropython, rust and tinygo programming languages on esp32 microcontroller. *Electronics, 12(1)*, 143, doi: https://doi.org/10.3390/electronics12010143.

[45] Mandana Sadat Ghafourian, Sara Tarkiani, Mobina Ghajar, Mohamad Chavooshi, Hossein Khormaei, and Amin Ramezani (2025). Optimizing warfarin dosing in diabetic patients through BERT model and machine learning techniques. *Computers in Biology and Medicine, 186*, 109755, doi: https://doi.org/10.1016/j.compbiomed.2025.109755.

[46] Sadik Kamel Gharghan and Huda Ali Hashim (2024). A comprehensive review of elderly fall detection using wireless communication and artificial intelligence techniques. *Measurement, 226*, 114186, doi: https://doi.org/10.1016/j.measurement.2024.114186.

[47] Nurul Amirah Mashudi, Syaidathul Amaleena Rossli, Norulhusna Ahmad, and Norliza Mohd Noor (2021). Breast Cancer Classification: Features Investigation using Machine Learning Approaches. *International Journal of Integrated Engineering, 13(5)*, 107-118, doi: https://doi.org/10.30880/ijie.2021.13.05.012.

[48] Dustin Scheinost, Stephanie Noble, Corey Horien, Abigail S Greene, Evelyn MR Lake, Mehraveh Salehi, Siyuan Gao, Xilin Shen, David O'Connor, and Daniel S Barron (2019). Ten simple rules for predictive modeling of individual differences in neuroimaging. *NeuroImage, 193*, 35-45, doi: https://doi.org/10.1016/j.neuroimage.2019.02.057.

[49] Murugadoss R (2021). Early Prediction of Diabetes Using Deep Learning Convolution Neural Network and Harris Hawks Optimization. *International Journal of Integrated Engineering, 13(1)*, 88-100, doi: https://doi.org/10.30880/ijie.2021.13.01.009.

[50] Pradeep Kumar Roy, Asis Kumar Tripathy, Tapan Kumar Das, and Xiao-Zhi Gao (2020). A framework for hate speech detection using deep convolutional neural network. *IEEE Access, 8*, 204951-204962, doi: https://doi.org/10.1109/ACCESS.2020.3037073.

[51] Chakkrit Tantithamthavorn, Ahmed E Hassan, and Kenichi Matsumoto (2018). The impact of class rebalancing techniques on the performance and interpretation of defect prediction models. *IEEE Transactions on Software Engineering, 46(11)*, 1200-1219, doi: https://doi.org/10.1109/TSE.2018.2876537.

[52] Davide Chicco and Giuseppe Jurman (2020). The advantages of the Matthews correlation coefficient (MCC) over F1 score and accuracy in binary classification evaluation. *BMC genomics, 21*, 1-13, doi: https://doi.org/10.1145/2939672.2939785.

[53] Giang Nguyen, Stefan Dlugolinsky, Martin Bobák, Viet Tran, Álvaro López García, Ignacio Heredia, Peter Malík, and Ladislav Hluchý (2019). Machine learning and deep learning frameworks and libraries for large-scale data mining: a survey. *Artificial Intelligence Review, 52*, 77-124, doi: https://doi.org/10.1016/j.nima.2017.06.020.

[54] Danielle F Eytan, Linda X Yin, Zahra Maleki, Wayne M Koch, Ralph P Tufano, David W Eisele, Kofi DO Boahene, Carole Fakhry, Justin A Bishop, and William H Westra (2018). Utility of preoperative fine needle aspiration in parotid lesions. *The Laryngoscope, 128(2)*, 398-402, doi: https://doi.org/10.1002/lary.26776.

[55] Davide Chicco, Valery Starovoitov, and Giuseppe Jurman (2021). The benefits of the Matthews correlation coefficient (MCC) over the diagnostic odds ratio (DOR) in binary classification assessment. *IEEE Access, 9*, 47112-47124, doi: https://doi.org/10.1109/ACCESS.2021.3068614.

Int. Journal of Integrated Engineering Vol. 18 No. 3 (2026) p. 366-388

[56] Wanqing Xiang, Haiying Rao, and Liyu Zhou (2020). A meta-analysis of contrast-enhanced spectral mammography versus MRI in the diagnosis of breast cancer. *Thoracic cancer, 11(6)*, 1423-1432, doi: https://doi.org/10.1111/1759-7714.13400.

[57] Huda Ali Hashim, Saleem Latteef Mohammed, and Sadik Kamel Gharghan (2020). Accurate fall detection for patients with Parkinson's disease based on a data event algorithm and wireless sensor nodes. *Measurement, 156*, 107573, doi: https://doi.org/10.1016/j.measurement.2020.107573.